International Journal on Advanced Science Engineering Information Technology

Vol.8 (2018) No. 6
ISSN: 2088-5334

Inner-Canthus Localization of Thermal Images in Face-View Invariant

Hurriyatul Fitriyah, Edita Rosana Widasari, Rekyan Regasari Mardi Putri

Department of Computer Engineering, University of Brawijaya, Malang, 65145, Indonesia
E-mail: hfitriyah, editarosanaw, rekyan.rmp@ub.ac.id

***Abstract*— Inner-canthus localization has played an essential role in measuring human body temperature. This is due to the theory that human core body temperature can be measured in the inner-canthus. Such measurement is useful for mass screening since it is non-contact, non-invasive and fast. This paper presents an algorithm that has been developed to locate the inner-canthus. The algorithm proposed a robust method in various face-view, i.e., frontal, sided and tilted. The algorithm consisted of: face segmentation, determining face-orientation, rotating face into straight view, eye localization, and inner-canthus localization. The face segmentation used human temperature threshold of 34°C — the face orientation used trend line of a middle point between each most-bottom and most-top coordinates. The face rotation was based on the gradient of the trend line. Once the face is rotated, the eye location was determined using facial proportion. The inner-canthus location was determined as the highest intensities in the eye-frame. The test on 15 thermal images of faces with various view showed localization accuracy of 80% for eye-frame determination and 100% for inner-canthus localization.**

***Keywords*— inner-canthus; thermal images; human body temperature; invariant.**

I. INTRODUCTION

During an epidemic of viral infection, body temperature was the first to be screened in public facilities — the fever result elevation on body temperature significantly above 37.3°C [1]. Research in average body temperature using axillary thermometer showed the temperature was between 36.2°C and 36.8°C [2]. Temperature above those ranges should be considered as having a fever. All countries have high anxiety about the dangerous disease will be epidemic in their country. One of the guarded locations is gates in the airport [3]. This area is the entrance of passengers from other countries which was suspected to be a carrier of the Avian Flu disease. Therefore, the thermal camera has been used widely to screen febrile condition in every airport [4], [5]. The thermal camera was operated to measure the infrared radiation from the passengers who are correlated with heat or temperature.

The inner-canthus location has played an essential role as one of location for human body temperature measurement [6].in recent standard IEC 80601-2-59, the inner-canthi region is the best spot for fever screening [7]. It is located in the inner-tip of eyes and near the nose. There are many issues over the measured temperature in the inner-canthus whether it is sufficient to represent the body temperature. However, it is an appropriate spot to identify human body temperature with non-contact, non-invasive, and fast fashion [8]–[10].

The localization could be performed manually. Several algorithms to automatically locate the inner-canthus in thermal images has been developed. It located inner-canthus using anthropometry knowledge where the distance between eyes are one-fifth the head-breadth [11]. Inner-canthus is in the inner tip of eyes. Hence both would have the distance. Two high temperature in the thermal image that has the specific distance was assigned as inner-canthus. Other method applied to eye detection before the inner-canthus [12]. Once eyes were detected using Haar classifier, acanthus searching is performed in the x-axis quarter region of eyes.

Identifying inner-canthus in thermal image is tedious. Compare to a visible image, facial features in the thermal image such eyes, nose, the mouth appears more blurry and vary in time. Multi-Modality Image Registration (MMIR) could be utilized to combine visible and thermal image to get better localization of inner-canthus [13]. A registration procedure combines detected edges of both images. Once the registered image was obtained, the inner-canthi was localized based on its location in the visible image. A Discriminative Response Map Fitting (DRMF)-based model was used to find the inner-canthi location in the visible image.

The searching for inner-canthus has also been investigated in a visible RGB image. The inner-canthus could be located using two knowledge which was apparently between the inner and outer region of canthus and bisector of canthus angle [14].

Moreover, in the real condition, the algorithm of inner-canthus localization in thermal images are required to resolve the various posed by people. Therefore, this paper proposed the detecting of inner-canthus localization of thermal images in face-view invariant. It is expected not to bind human for specific frontal pose during non-contact measurement. Researches in face recognition of thermal images with various head pose used moment invariant [15] and Convolutional Neural Network (CNN) [16] without changing head's orientation. While the algorithm developed to determine head orientation [17], finding the orientation can be used to rotate or translate images into the desired view. Although the algorithm worked on the visible RGB image, it gave an insight on how to find face's orientation. It used facial features such as eyes, nose, and lips to determine the angle of pitch, yaw, and roll of the head. Similar to the study, [18] also develop an algorithm to determine head orientation by locating facial features such as eyebrows, eyes, nose, and mouth.

This paper proposed a knowledge-based algorithm to locate inner-canthus in thermal images in various face-view. The knowledge was applied using a simple and ordinary mathematical equation.

II. Material and Method

The algorithm was developed to handle variation on face view, i.e., frontal, side and tilted. The faces should not wear head accessories such as glasses, a scarf or hat. Infrared radiation does not pass through glasses. Hence inner-canthus would be invisible in the images. Scarf and hat would be left some part of the face to be unexposed, hence would not be adequately detected.

A. Data Acquisition

The thermal images were taken using FLIR i7 which senses infrared signal in spectral range 7.5 – 13 µm (long-wave infrared). It produces thermal images in 240x240 pixel and JPG format as shown in Fig. 1. The data were acquired in camera setting as follow:

- Face-to-camera distance is fixed in 1 m. This is due to the camera operation that requires a minimum of 0.6 m face-to-camera distance. A longer distance (>1 m) was not investigated in the study. This is due to low camera resolution, hence face details would be blurred.
- Colour palette was set to grayscale. This is due to the image processing technique utilized in the study used grayscale color-space, hence no color conversion would be required.
- The temperature range was locked in 24^0C - 39^0C. This follows temperature range of the human body and room.

Fig. 1 Image acquired using Thermal Camera

The acquired images were then cropped to discard unnecessary information that would not be analyzed further, i.e., temperature and camera brand.

The algorithm was developed to locate inner-canthus of a face with no challenge in the background. Henceforth there was no other heat-source within the range of human body temperature in the background. The only face of one person was acquired in a frame. There was no challenge in face accessories as well, e.g., putting-on hat, wearing scarf and glasses. Each face was acquired in 5 different face-views, which are:

View 1: Straight, Frontal
View 2: Straight, Right-sided
View 3: Straight, Left-sided
View 4: Right-tilted, Frontal
View 5: Left-tilted, Frontal

The degree of the face which was sided to the right and left was limited since a significant degree would make the inner-canthus unseen. The degree of the face which was tilted to the right and left was limited since a significant degree was uncommon to happen.

B. The algorithm of Inner-Canthus Localization in Various Face-View

The image processing steps of the developed algorithm are shown on Fig.2. The main idea of the algorithm was to found the straight view of various face-view. The straight view was important since eyes and inner-canthus would be easily located using a facial proportion of normal face. The algorithm first segment the face from the background based on knowledge of face. It then calculated the degree of face's tilted-angle which is necessarily required to rotate the face into straight view.

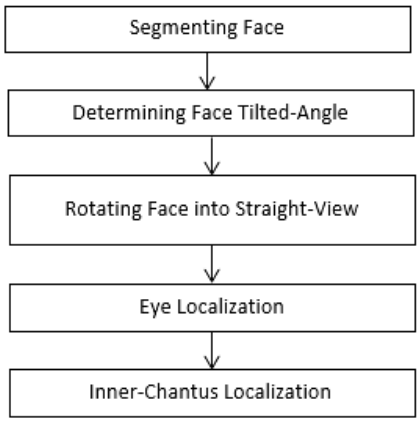

Fig. 2 Flowchart of Algorithm

1) Face Segmentation: for face segmentation from the background, two criteria of adult's face were used: (1) Temperature threshold of above 34^0C, (2) Minimum area of 647.9 cm2. Both criteria were based on knowledge of faces.

- Temperature Threshold > 34^0C.
  The first segmentation utilized simple Thresholding method that would assign binary number into an image. The algorithm used face temperature as a threshold to segment a face from non-face. The face

usually falls in the temperature range of above 34^{0}C since the thermal images were taken in the temperature range of 24^{0}C - 39^{0}C which equals to 0-255 grayscale intensity. Hence the temperature threshold used was 170. Fig. 3(a) shows the original image acquired while Fig. 3(b) shows the segmentation result based on temperature threshold.

(a) (b)

Fig. 3 Face Segmentation Based on Temperature; (a) Original Image, (b) Segmented face based on Temperature

- Area Threshold > 647.9 cm2.
  The minimum size of adult's head was 13.3 cm width and 15.5 cm height [19]. Since the human head is an oval shape, hence the area was found to be 647.9 cm2. This area was then converted in pixel size using the fact that pixel to actual ratio is 1:2. Henceforth, the minimum area of the face was 2620 pixel. Each connected components in the detected face based on the first criteria (as shown in Fig. 3(b)), which are less than 2620 pixel were then eliminated. Fig. 4(a) shows the original image, while Fig. 4(b) shows the segmented face based on temperature threshold and area threshold criteria.

(a) (b)

Fig. 4 Face Segmentation Based on Area; (a) Original Image, (b) Segmented Face based on Area

2) Determining Face Tilted-Angle: Tilted-angle of faces needs to be calculated in order to determine whether the face was tilted or straight. This straight view is essential since the facial proportion used to determine the eye location was based on the proportion of straight face. The tilted-angle was determined based on the gradient of vertical middle-points' trend line. This method is proposed to be simple without detecting facial features beforehand. The steps for determining the angel are listed below:

- Lists coordinates of most-top and the most-bottom edge of the segmented face
- Calculate coordinates of middle-point x_n, y_n between those most-top and most-bottom coordinates
- Operate polynomial fitting of second order to attain gradient, m, of trend-line for the vertical middle point using Equation (1) where N is the number of middle-point coordinates.

$$m = \frac{N\sum_{n=1}^{N} x_n y_n - \left(\sum_{n=1}^{N} x_n\right)\left(\sum_{n=1}^{N} y_n\right)}{N\sum_{n=1}^{N} x_n^{\,2} - \left(\sum_{n=1}^{N} x_n\right)^2} \quad (1)$$

- The tilted-angle was then defined using Equation (2).

$$tiltedAngle = \tan^{-1}(m) \quad (2)$$

Fig. 5(a) shows the segmented face while Fig. 5 (b) show the face orientation found. The middle-points coordinates are shown as a dot, and the trend-line is shown as a line.

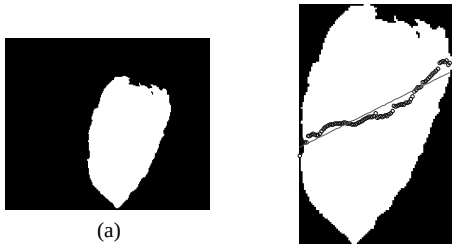

(a) (b)

Fig. 5 Determining Tilted-Angle; (a) Segmented Face, (b) Trend-line of face orientation

3) Rotating Face into Straight-View: The tilted-angle found was then used to rotate the segmented faces into straight view. The rotation used the opposite direction from the tilted-angle using Equation (3). The negative sign would rotate the segmented face in exact opposite angle counterclockwise if the gradient were positive and clockwise if the gradient was negative to result in 0° angle of the face (straight view). Fig. 6(b) shows the rotating result into a straight view of the original image in Fig. 6(a).

$$rotationAngle = -(tiltedAngle) \quad (3)$$

(a) (b)

Fig. 6 Rotating Face; (a) Original Image, (b) Rotated Face into Straight View

4) Eye Localization: Inner-canthus show the highest temperature in the face. Nevertheless, the highest temperature was not only found in inner-canthus. Several spots in the face such forehead, nose-tip and mouth-tip in several faces show the highest temperature as well. Fig. 7 shows several spots in the face that has high temperature shown as an asterisk (*).

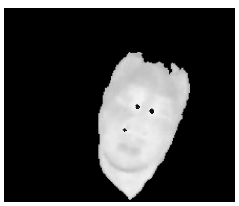

Fig. 7 The highest temperature appears in inner-canthus and nose-tip

Since several spots in the face have the highest temperature similar to inner-canthus, directly assigning the highest intensity as inner-canthus could lead to false detection. An eye localization is required to narrow the searching area where the highest temperature only appears in inner-canthus.

Once the face is rotated into straight-view, the eye location was found based on the facial proportion of straight face. The face-box was determined beforehand based on facial proportion as well.

- Face-Box Determination: Face Box is a frame that was based on the human facial proportion of height/width which is 1.6 [20]. The first edge determined was left and right edge. These vertical edges were calculated as the most-left vertical coordinate for left-edge and most-right vertical coordinate for right-edge. The face width was the distance between left-edge and right-edge. The top-edge was determined as the most-top horizontal coordinate. The bottom-edge was determined based on facial proportion where it was 1.6 of face width from the top edge. Fig. 8 shows the detected Face-box which is shown as the black rectangle that binds and crops the segmented face.

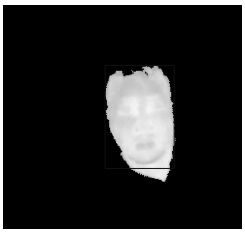

Fig. 8 Face-Box

- Eye-Frame Determination: Once the face-box was found, the eye location was determined based on facial proportion where it located in the border between the first and second upper one-third of face height [12]. The eye frame was then decided to be located within ± 0.5 from the border. Eye-frame detected as shown in Fig. 9 as a box.

5) Inner-Canthus Localization: Based on the theory, inner-canthus was the highest temperature in the inner corner of the eye. This fact was used in the algorithm to determine the inner-canthus location as coordinate/s of the highest intensity in the eye-frame. This method is simple since no template was required. Fig. 9 shows the eye-frame (box) and inner-canthus location (asterisk,*). In Fig. 9, the inner-canthus appears as blob-like since more than one pixels were indicated to having the highest intensity.

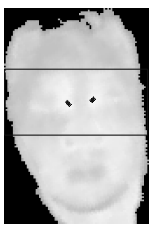

Fig. 9 Eye-Frame (box) and Inner-Canthus Location (asterisk,*)

III. Result and Discussion

The algorithm was tested in 15 images from 3 people acting 5 different face-views. The Thresholding method which was based on temperature was an accurate and straightforward way to detect a face. Chest area had a similar temperature to the face, but since it was mostly covered in public by clothes, the infrared radiation is reduced to travel through. The chest area appeared to have lower intensity in the thermal image compare to face. The temperature in the face was also distinctive in the public environment as it appears brighter due to the high temperature of the human body. Human also has homeostatic regulation that keeps its temperature within a specific range, hence faces in non-extreme condition would still be detected using the defined temperature threshold.

Face area as second criteria was able to detect a face from area candidates that fall within the defined range of temperature. It eliminated some part of the chest that was false-segmented in the binary image. Human's anthropometry is standard for every normal head. Hence it was accurate to detect a face using the simple calculation of the area.

The algorithm accuracy deeply depended on the face-rotation process. The gradient which was found using the polynomial fitting of second order was able to determine head-orientation as shown in Fig. 10. During pose 1, 2 and three which is shown in the three upper part of Fig. 10, the gradient of trend-line was little meaning it was in straight-position which was accurate since the face was not tilted. While for the two lower images in Fig. 10, both faces were tilted at a certain degree, and it can be seen that the gradient of trend-line is high. The trend line also showed head-orientation of different tilted-angle.

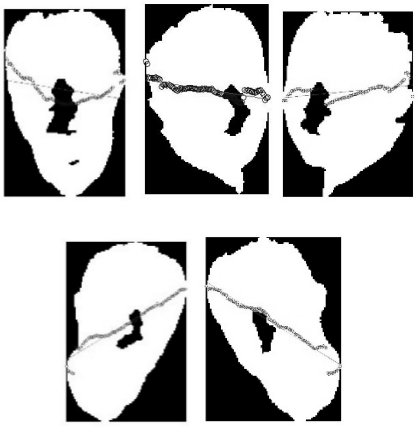

Fig. 10 Trend-line in various face-view

Figure 10 above shows that the face-rotation algorithm was also affected by the presence of neck. It is an exposed body part as well. Hence it fell within the range of temperature in the segmentation process and was considered as a face. The trend-line in face-view 1 (top, left-most in Fig. 10) is slightly tilted since the middle-points in the center were calculated between the top of head and bottom of the neck. The result of face-rotation for face-view 1 in Figure 10 is shown in Figure 11. The result is the head was slightly rotated.

(a) (b)

Fig. 11 Face-rotation for face-view 1, straight and frontal; (a) Original Image, (b) Rotated Face

The face-rotation process was specially designed for face-view 4 and five which were tilted head. The rotation used a negative value of the tilted-angle to rotate the face into straight view. The result for all pose 4 and five from 3 test people are shown in Fig. 12. Each row in Fig 12 is the result of a person where left-images are for left-tilted, and right-images are for right-tilted. Each image is a pair of original image and its rotation result. The rotation was able to rotate tilted-face into straight position as shown in Fig.12.

Fig. 12 Result of Face Rotation for Pose 4 and Pose 5

The facial proportion helped the algorithm to determine face-box and eye-frame in a simple calculation. The result of detected face-box and eye-frame from 15 images is shown in Fig. 13 in every right side of its original images. Fig. 13 also shows the result of eye-frame which is indicated as a rectangle and inner-canthus which is indicated as an asterisk (*).

The face-box determination was based on the golden ratio of 1.6. The ratio was primarily used to determine the height of the face and cropped the lower part of the segmented image to eliminate neck area. In Fig. 13, all face-box still has neck area included. Ears are also shown in several face-box. The lower ratio could be implemented to eliminate the non-face area. Other statistical parameters could also be used instead of the out-most coordinate to be assigned as the edge of the face's bounding-box.

Accuracy for eye-frame and inner-canthus of all 15 images is listed in Table 1. Result for localization from the algorithm was compared to manual. The accuracy for eye-frame detection was 80%, while inner-canthus detection was 100%. In Image ID 2c, 2d, and 2e, only lower part of eyes were detected within eye-frame. The condition was affected by the presence of a neck in the fare-box. Face-height was longer than it should be. Hence eye-frame position in some images was descended.

TABLE I
THE ACCURACY OF EYE-FRAME AND INNER-CANTHUS LOCALIZATION

ID	**Detection Result**	
	Eye-Frame	**Inner-Canthus**
1a	1	1
1b	1	1
1c	1	1
1d	1	1
1e	1	1
2a	1	1
2b	1	1
2c	0	1
2d	0	1
2e	0	1
3a	1	1
3b	1	1
3c	1	1
3d	1	1
3e	1	1
Accuracy	**80%**	**100%**

- 1 = accurate location, 0 = false location

Fig. 13 Result of Face-box, Eye-frame, and Inner-canthus of Test Images

Eye-frame was low in some images, inner-canthus localization still results in an accuracy of 100%. This is due to the location of inner-canthus which is in the inner-tip of an eye. The tip is in the middle compared to eye-height. Hence it was still located accurately. Locating inner-canthus by searching maximum intensity within eye-frame was then accurate. There was no other spot in the eye-frame which has the highest intensity except the inner-canthus. Moreover, this localization process requires an only a simple method by searching the maximum intensity within the eye-frame in Image ID 1b, 1e, 2a, 2b, and 3d, inner-canthus appear in more than one pixel. It appears as a blob-like region in inner-canthus location.

The algorithm has accurately detected inner-canthus. Nevertheless, mostly only one inner-canthus of eyes were detected. Left and a right eye appeared to have a slightly different temperature. Since only the maximum intensity was assigned as inner-canthus, both inner canthus in most images were not detected. For temperature measurement, this one detected inner-canthus is sufficient to represent the temperature of the human body. The measurement chooses the highest temperature between both inner-canthus.

For inner-canthus detection purpose, the highest temperature as main criteria could be expanded not to only its maximum value but several high temperatures. Thus other inner-canthus which have lower intensity could still be detected.

IV. Conclusions

In this paper, an algorithm to locate inner-canthus has been developed. The localization process was based on two knowledge where eyes are in a particular location of face height based on facial proportion, and inner-canthus has the highest temperature that was implemented using simple calculation. This paper also has proposed gradient of trend line from vertical middle-points to determine face-orientation. Further study should include facial challenges

such as head accessories and another heat-source in the background to result in more adaptive non-contact measurement algorithm of human body temperature.

REFERENCES

[1] S. Kumar, C. Chandra C. "Supply Chain Disruption by Avian flu pandemic for U.S. companies: a case study," *IEEE Eng. Management Rev*, vol. 44, pp. 65-73, 2016.

[2] S. Marui, A. Misawa, Y. Tanaka, K. Nagashima. "Assessment of Axillary Temperature for the Evaluation of Normal Body Temperature of Healthy Young Adults at Rest in a Thermoneutral Environment." *Jour. of Physiological Anthropology*. Vol. 36 (18), 2017.

[3] K.M. Gostic, A.J. Kucharski, J.O. Lloyd-Smith. "Effectiveness of Traveller Screening for Emerging Pathogens Is Shaped by Epidemiology and Natural History of Infection." Ed. S.I. Hay. *eLife*, vol. 4, 2015

[4] Y. Nakayama, G. Sun, S. Abe, "Non-contact Measurement of Respiratory and Heart Rates using CMOS Camera-equipped Infrared Camera for Prompt Infection Screening at Airport Quarantine Stations," in *Proc. IEEE Int. Conf. on Comp. Intelligence and Virtual Env. for Measurement Syst. and App*, 2015.

[5] L.A. Selvey, C. Antão, R. Hall R. "Evaluation of Border Entry Screening for Infectious Diseases in Humans." *Emerg Infect Dis*. Vol. 21(2), pp. 197-201, 2015.

[6] R. Vardasca, A.R. Marques, J. Diz, A. Seixas, J. Mendes, E.F.J. Ring, (2017). "The Influence of Angle and Distance on Temperature Readings from the Inner-Canthi of the Eye." *Thermology Int.*, vol. 27, pp. 130-135. 2017.

[7] *IEC 80601-2-59: Particular Requirements for the Basic Safety and Essential Performance of Screening Thermographs for Human Febrile Temperature Screening*, International Electrotechnical Commission (IEC)/International Organization for Standardization (ISO), 2017.

[8] S. Budzan, R.Wyzgolik, "Face and Eyes Localization Algorithm in Thermal Images for Temperature Measurement of the Inner Canthus of the Eyes," *Infrared Phys. and Tech. Jour.*, vol. 60(1), pp. 225-234, 2013.

[9] T. Y. Su *et al.*, "Noncontact detection of dry eye using a custom designed infrared thermal image system," *J. Biomed. Opt.*, vol. 16, no. 4, p. 46009, 2011.

[10] E.G., Zahran, A.M. Abbas, M.I. Dessouky, M.A. Ashour, K.A. Sharshar, "Performance Analysis of infrared face recognition using PCA and ZM," in *Proc.* IEEE *ICCES*, 2009.

[11] B. Amanda, "Detection and Tracking in Thermal Infrared Imagery," Thesis, Linköping University, Linköping, Sweden, 2016.

[12] N.I.N. Ishak, J.M. Desa, W.W. Kit, L.H.Siong, 'Fuzzy Logic Base Viola Jones Fever Detection Method in Thermal Imaging System", in *Proc. IISRO*, 2013

[13] Y.N. Dwith Chenna, P. Ghassemi, T.J. Pfefer, J. Casamento, Q. Wang, "Free-Form Deformation Approach for Registration of Visible and Infrared Facial Images in Fever Screening." *Sensors*. Vol. 18 (125), 2018.

[14] J.P. Batista. "Locating Facial Features Using an Anthropometric Face Model for Determining the Gaze of Faces in Image Sequences." *ICIAR*, LNCS 4633, pp. 839-853, 2007.

[15] N. Zaeri, "Pose Invariant Thermal Face Recognition Using AMI Moments," in *Proc. UKSim-AMSS 18th Int. Conf. on Comp. Model. and Sim.*, 2016

[16] Z. Wu, M. Peng, T. Chen, "Thermal Face Recognition using Convolutional Neural Network," in *Proc. Int. Conf. on Optoelectronics and Image Process. (ICOIP)*, 2016.

[17] D. Dervinis, "Head Orientation Estimation using Characteristic Points of Face," *Elektronika in Elektrotechnika*, vol. 8(72), pp. 61-64, 2006

[18] C.Xui, Y. Zheng, Z. Wang, "Semantic feature Extraction for Accurate Eye Corner Direction," in. *Proc. ICPR*, 2008.

[19] *Anthropometry and Biomechanics*, Man-System Integration Standard, Vol. 1 Section 3., NASA-STD-3000, Revision B, 1995.

[20] P.M. Prendergast, *Facial Proportions*, ser. Advanced Surgical Facial Rejuvenation, Berlin: Germany, Springer, 2012.